



Removal of nitrate and Cr(VI) from drinking water by a macroporous anion exchange resin

Yuanyuan Ye^a, Yongxiang Ren^{a,*}, Jing Zhu^a, Junping Wang^a, Bangyan Li^b

^aKey Laboratory of Northwest Water Resource Environment and Ecology, Ministry of Education, Shaanxi Key Laboratory of Environmental Engineering, School of Environmental and Municipal Engineering, Xi'an University of Architecture and Technology, Xi'an 710055, China, Tel. +86 13609208237; email: cynthiayyy@qq.com (Y. Ye), Tel. +86 13619215317; Fax: +86 029 82202729; emails: ryx@xauat.edu.cn (Y. Ren), zhujingfeiyang@163.com (J. Zhu), wangjunping@xauat.edu.cn (J. Wang)

^bCollege of Architecture, Xi'an University of Architecture and Technology, Xi'an 710055, China, email: bylea@qq.com

Received 12 September 2015; Accepted 3 March 2016

ABSTRACT

Nitrate and hexavalent chromium (Cr(VI)) are potentially hazardous to human health and ecosystems. In this study, an anion exchange resin (PBO-8) was synthesized for the removal of nitrate and Cr(VI) from aqueous solution. The PBO-8 resin was characterized with Fourier transform infrared spectroscopy, scanning electron microscopy and BET surface area analyses. The results of batch adsorption experiments indicated that the maximum equilibrium uptake of nitrate and Cr(VI) in single solute solutions were 21.13 and 45.02 mg/g, respectively. The maximum quantity of PBO-8 resin for the adsorption of nitrate and Cr(VI) were, respectively, decreased to 14.17 and 27.03 mg/g in a nitrate and Cr(VI) binary solution. The increase in temperature and decrease of pH enhanced the capacity of the PBO-8 resin for Cr(VI) adsorption, but such effects were less significant for nitrate. The Gibbs free energy change, enthalpy change, and entropy change illustrated that the adsorption of aqueous nitrate and Cr(VI) were feasible, endothermic, and spontaneous. Furthermore, the behaviors of the nitrate and Cr(VI) adsorption onto the PBO-8 resin showed a better fit to the Langmuir isotherm and pseudo-second-order kinetic models. Intraparticle diffusion was the rate-limiting step.

Keywords: Nitrate removal; Cr(VI) removal; Drinking water; Anion exchange resin; Rate-limiting step

1. Introduction

In recent years, nitrate and hexavalent chromium (Cr(VI)) have emerged as drinking water pollutants. These two anionic pollutants can occur together in water resources as nitrate is a common co-contaminant in surface and ground waters [1]. Excessive nitrate concentration in drinking water may cause

methemoglobinemia in infants, and human gut cancer as nitrate is reduced to nitrite [2,3]. Considering the harmful effects of nitrate on the human body, the World Health Organization (WHO) set 10 mg/L nitrate-nitrogen as the permissible limit in drinking water [4]. The nitrate concentrations in groundwater usually reach 40–50 mg L⁻¹ in France, Russia, Netherlands, and America, and are even as high as 500–700 mg L⁻¹ in other places [5–7]. The situation of

*Corresponding author.

nitrate pollution in China is not optimistic. Investigations at 641 sites in 8 provinces in northern China showed that 73.8% of groundwater could not be used as a resource for drinking water in 2009; the main pollutants included nitrate [8]. Chromium contamination of soil, surface, and ground water is a worldwide problem because of its widespread use in many industrial applications such as the production of stainless steel, chrome plating, leather tanning, and wood treatment [1,9]. Cr(VI) is of more concern as it is highly toxic and soluble in water, mutagenic and carcinogenic to living organisms [1,9,10]. The amount of Cr(VI) in the drinking water resources of some cities in China exceed the maximum allowable chromium concentration in drinking water [8], which has been set to 0.05 mg L^{-1} by the WHO [11]. Moreover, in a groundwater quality survey of 48 wells at the Jinghuiqu irrigation district in the Shaanxi province of China, the concentration of Cr(VI) in 55.32% of the groundwater samples exceeded 0.05 mg L^{-1} . Values as high as 0.535 mg L^{-1} were recorded in some samples, which is nearly 11 times higher than the set standard.

The treatment methods available for anionic pollutants removal from aqueous solution include biological (microbial) remediation [12,13], adsorption [14,15], chemical reduction, reverse osmosis, electrodialysis, and ion exchange [4]. The biological denitrification method is not sufficient to treat water polluted with low concentrations of nitrate, especially under the condition of carbon source shortage. In addition, there are some limitations owing to the contamination of drinking water with germs and metabolic substances. Furthermore, biological (microbial) Cr(VI) removal from drinking water is greatly influenced by seasonal and natural environmental conditions. Therefore, it is difficult to obtain a stable treatment effect. Inorganic materials such as activated carbon and other minerals have been utilized as adsorbents for removal of various contaminants. However, due to the production of excess waste, low mechanical strength, and regeneration rate, the cost of operation and waste disposal often gets higher with these processes. Although the chemical reduction of Cr(VI) and nitrate with the use of zero-valent or ferrous iron is quite efficient [16], the main disadvantages of the process are the high cost of chemicals, secondary contamination of the water and the production of large volumes of sludge. Thus, the ion exchange process, with its simplicity, effectiveness, relatively low cost, and chemical stability [4,17] seems to be the most practical method for water purification and removal of anionic pollutants from drinking water. Consequently, studies on novel adsorbents based on the ion exchange method are attracting global interest, in terms of its practical application.

Triethanolamine is a dual-natured compound of both amines and alcohols. It is an excellent chelate reagent, which can generate 2–4 ligands with a variety of metal ions. Its application is significantly limited by its liquid form at room temperature. Therefore, the immobilization of triethanolamine on a polymer would expand its application range. In this study, a macroporous anion exchange resin with both chelate and exchangeable functional groups, PBO-8, was formulated via polymerization, chloromethylation by 1,4-bis(chloromethoxy) butane, followed by quaternarization using triethanolamine. The advantages of chloromethylation reagent, 1,4-bis(chloromethoxy) butane, have been reported in our previous work [18]. The physicochemical properties of PBO-8 resin were characterized, the equilibrium and kinetic parameters for nitrate and Cr(VI) adsorption from aqueous solution were investigated. Also, the effects of competing anions on nitrate and Cr(VI) removal were evaluated.

2. Materials and methods

2.1. Materials

The monomers to be polymerized were styrene (ST, 99%) and divinylbenzene (DVB, containing 80% DVB isomers, the remainder mainly being 3- and 4-ethylvinylbenzene). Styrene was supplied by Kermel Chemical Reagent Co., Ltd (Tianjin, China) and DVB was provided by Jingchun Scientific Co., Ltd (Shanghai, China). Prior to polymerization, both the monomers were pre-treated to remove the inhibitor, 4-tert-butylcatechol (TBC). The initiator, benzoyl peroxide (BPO, 99%, remainder water), was supplied by Fuchen Chemical Reagent Co., Ltd (Tianjin, China). 1,4-bis(chloromethoxy) butane (BCMB, 99%) was supplied by Langene Bio-science Co., Ltd (Xi'an, China) and used as the chloromethylation reagent. The catalyst for the chloromethylation reaction, anhydrous stannic chloride was provided by Sinopharm Chemical Reagent Company (China). All other reagents were of analytical grade and obtained from Kermel Chemical Reagent Co., Ltd, and used without further purification. Deionized water was used to prepare the aqueous solutions.

2.2. Preparation of PBO-8 resin

The macroporous anion exchange resin named as PBO-8 was prepared via a three-stage reaction, which consist of suspension polymerization [19], chloromethylation, and quaternarization. The details of the process are described below: a 2-L glass

reaction kettle equipped with a thermometer, a reflux condenser, and a mechanical stirrer was charged with 725.8 mL (2.5%) polyvinyl alcohol and 181.4 mL (2%) gelatine solution. The mixture was heated to 60°C. Meanwhile, 240 mL of ST, 12 mL of DVB, 201.6 mL of liquid paraffin, and 2.27 g of BPO were mixed and then added to the former solution. Subsequently, the glass reaction kettle was heated at 95–100°C with continuous stirring at 170 rpm for 10 h. Poly(styrene-divinylbenzene) particles (PSM) were obtained by filtration and were extracted with ethanol for 8 h in a Soxhlet apparatus. Next, 20 g of PSM was first swollen in the mixture of dichloromethane (200 mL) and BCMB (36 g) for at least 1 h. Then 20 mL of anhydrous stannic chloride was added. The reactant mixture was stirred at 150 rpm for 6 h at room temperature. Subsequently, the chloromethylated poly(styrene-divinylbenzene) particles (CPSM) were filtered and washed with dilute hydrochloric acid, 1,4-dioxane, distilled water, and alcohol, respectively. Finally, PBO-8 resin was obtained by the quaternarization of CPSM (20 g) with triethanolamine (182 mL) in dimethyl sulfoxide (100 mL) at 95–100°C for 24 h.

2.3. Batch adsorption experiments

Batch adsorption experiments were carried out in 150 mL conical flasks by putting a specified amount of the PBO-8 resin in contact with 50 mL of solution. The solutions were poured into flasks after the addition of the resin, and shaken at a constant speed of 150 rpm in an oscillating incubator (BS-2F, Jintan, China). The details of the batch experimental procedure were described in detail by Samatya and Milmile [4,20].

A nitrate adsorption kinetics study was carried out using a fixed resin dose of 0.15 g resin/50 mL of solution and an initial nitrate concentration of 100 mg-N L⁻¹. The nitrate concentration was subsequently measured at predetermined time intervals of 0–150 min at 25°C. Furthermore, a nitrate adsorption isotherm study was carried out using a fixed resin dose of 0.15 g resin/50 mL of solution and different initial nitrate concentrations of 5, 10, 15, 20, 40, 60, 80, 100, 150, and 200 mg-N L⁻¹ at 25°C for 24 h. To determine the optimum quantity of resin for nitrate removal from aqueous solution, the resin dose was varied from 0.1 to 0.8 g resin/50 mL of solution (100 mg-N L⁻¹). All other parameters were kept constant. The effect of temperature on nitrate removal was evaluated using a fixed resin dose of 0.15 g resin/50 mL of solution, and an initial nitrate concentration of 100 mg-N L⁻¹. The effects of increased competing anions (SO₄²⁻, Cl⁻, CO₃²⁻, HCO₃⁻, and F⁻) on nitrate adsorption by the PBO-8 resin

were investigated. The concentration of nitrate (100 mg-N L⁻¹) was kept constant, and the dose of resin was fixed at 0.15 g/50 mL of solution.

The Cr(VI) adsorption kinetics study was performed using a fixed resin dose of 0.1 g resin/50 mL of K₂Cr₂O₇ solution and an initial Cr(VI) concentration of 100 mg-Cr L⁻¹. The Cr(VI) concentration was subsequently measured at predetermined time intervals of 0–36 h at 30°C. The Cr(VI) adsorption isotherm study was carried out with a fixed resin dose of 0.1 g resin/50 mL of solution using different initial Cr(VI) concentrations of 5, 10, 15, 20, 40, 60, 80, 100, 150, and 200 mg-Cr L⁻¹ at 30°C for 32 h. To determine the optimum quantity of resin for Cr(VI) removal from aqueous solution, the dose of resin was varied from 0.1 to 0.8 g resin/50 mL of solution (150 mg-Cr L⁻¹). All other parameters were kept constant. The effect of temperature on Cr(VI) removal was evaluated at a fixed resin dose of 0.1 g resin/50 mL of solution (100 mg-Cr L⁻¹). The effects of increased competing anions (SO₄²⁻, Cl⁻, CO₃²⁻, HCO₃⁻, and NO₃⁻) on Cr(VI) adsorption on the PBO-8 resin was investigated by keeping the concentration of Cr(VI) (100 mg-Cr L⁻¹) constant, and the dose of resin was fixed at 0.1 g/50 mL of solution.

Binary adsorption studies of nitrate and Cr(VI) by the PBO-8 resin were performed at 25°C for 24 h. A synthetic binary solution was prepared by mixing nitrate and Cr(VI). To determine the optimum amount of resin required for nitrate and Cr(VI) removal from the binary solution, the dose of resin was varied from 0.1 to 0.8 g resin/50 mL of binary solution. The initial concentration of nitrate and Cr(VI) in binary solution were both 100 mg L⁻¹. The impact of initial concentration on nitrate and Cr(VI) adsorption was carried out at a fixed resin dose of 0.3 g resin/50 mL of binary solution. Initial concentrations of nitrate (Cr(VI)) in the binary solution were 5, 10, 20, 40, 60, 80, 100, 150, and 200 mg L⁻¹, respectively. All other parameters were kept constant. The Cr(VI) and nitrate adsorption kinetics studies were carried out using a fixed resin dose of 0.3 g resin/50 mL of binary solution. Nitrate and Cr(VI) concentrations were analyzed at predetermined time intervals of 0–24 h. Initial concentrations of nitrate and Cr(VI) in the binary solution were both 100 mg L⁻¹.

Desorption studies of nitrate and Cr(VI) by the PBO-8 resin were performed at 25°C. The adsorption quantity of nitrate and Cr(VI) of regenerated resin was determined via the repetition of adsorption experiments. The nitrate adsorption experiments were carried out using a fixed resin dose of 0.15 g resin/50 mL of nitrate solution and an initial nitrate concentration of 100 mg-N L⁻¹. The Cr(VI) adsorption experiments were carried out using a fixed resin dose of 0.1 g resin/50 mL of Cr(VI) solution and an initial Cr(VI)

concentration of 100 mg-Cr L⁻¹. To determine the effects of contact time on the desorption of nitrate and Cr(VI), the saturated resin was specified in the same dose as their adsorption experiments. All other parameters were kept constant.

2.4. Column adsorption experiments

Studies on the column adsorption performance were carried out using a glass column with an inner diameter of 2.5 cm at room temperature. PBO-8 resin of 20 g was packed into the glass column at 15 cm. The nitrate solution with an initial concentration of 50 mg-N/L was continuously passed through the column at a flow rate of 27 mL/min. Samples were collected at the bottom of the column at regular intervals.

2.5. Adsorption models and calculation formulas

The amounts adsorbed at equilibrium (Q_e , mg g⁻¹) were calculated by Eq. (1) [4]:

$$Q_e = \frac{V(C_0 - C_e)}{W} \quad (1)$$

The experiment results of the nitrate and Cr(VI) adsorption isotherms were further correlated by the Langmuir (Eq. (2)), Freundlich (Eq. (3)), and D-R adsorption (Eq. (4)) isotherm models [4,21]:

$$Q_e = \frac{Q_0 b C_e}{1 + b C_e}, \quad r = \frac{1}{1 + b C_0} \quad (2)$$

$$Q_e = K_f C_e^{(1/n)} \quad (3)$$

$$\ln Q_e = \ln Q_0 - \beta' \varepsilon^2, \quad \varepsilon = RT \ln \left(1 + \frac{1}{C_e} \right), \quad (4)$$

$$E = \frac{1}{(2\beta')^{1/2}}$$

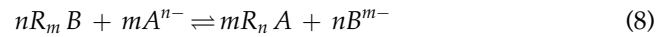
Kinetic data for PBO-8 resin were then represented by the pseudo-first-order model (Eq. (5)), the pseudo-second-order model (Eq. (6)), [22] and the Elovich model (Eq. (7)) [23]:

$$\ln \frac{Q_e - Q_t}{Q_e} = -K_1 t + A \quad (5)$$

$$\frac{t}{Q_t} = \frac{1}{K_2 Q_e^2} + \frac{t}{Q_e}, \quad h = K_2 Q_e^2 \quad (6)$$

$$Q_t = \frac{1}{\beta} \ln(\alpha\beta) + \frac{1}{\beta} \ln t \quad (7)$$

The anion exchange reaction in PBO-8 resin can be written as:



The selectivity coefficients were calculated by Eq. (9) [24].

$$K_B^A = \frac{[X_A]^m \cdot [B]^n}{[X_B]^n \cdot [A]^m} \quad (9)$$

where $[X_A]$ and $[X_B]$ are the molarities of A and B anions in the resin at equilibrium; $[A]$ and $[B]$ are the molarities of A and B anions in the external aqueous solution at equilibrium, respectively.

2.6. Resin characterization and anions analysis

The surface physical morphology of the PBO-8 resin was observed under a scanning electron microscope (SEM) (JEOL, JSM-6510LV, Japan). The surface functional groups of PSM, CPSM, and the PBO-8 resin were detected by a Fourier transform infrared (FTIR) spectrometer (Shimadzu, IRPrestige-21, Japan), where the spectra were recorded in the wave number ranging from 400 to 4,000 cm⁻¹. N₂ adsorption–desorption tests were carried out at 77.35 K to determine the specific surface area and pore size distribution based on the BJH model using an automated surface area and pore size analyzer NOVA 4200e (Quantachrome Instruments corp., US). Nitrate-nitrogen was analyzed using a UV spectrophotometer (STECH, 752 N, China) at a wavelength of 220 nm. One mL of 1.0 N HCl and 0.1 mL of 0.8 wt.% sulfamic acid were added to 50 mL of sample in order to eliminate the interface of organic ions and nitrite, respectively. Cr(VI) was determined using the UV spectrophotometer at a wavelength of 540 nm. The principle for measuring Cr(VI) was based on the chromogenic reaction of Cr(VI) with diphenylcarbazide in an acidic condition.

3. Results and discussion

3.1. Characterization of PBO-8 resin

Fig. 1(a), (b), and (c) are the SEM images of the PBO-8 resin at magnifications of 50×, 2,000×, and 10,000×, which indicate that the synthesized resin

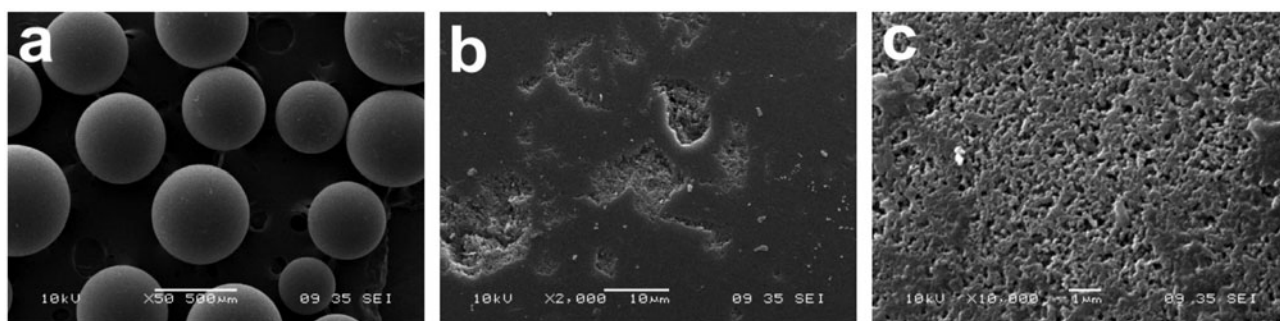


Fig. 1. SEM images of PBO-8 resin at the magnification of (a) 50 \times , (b) 2,000 \times , and (c) 10,000 \times .

consisted of spherical particles with uniformly distributed holes. The absorption peaks marked as PSM (Fig. 2) were the qualitative characteristic absorption peaks of the styrene-divinylbenzene copolymer. The peak at 1,600 cm^{-1} belongs to an aromatic ring. By comparing with PSM, the three strong characteristic peaks appeared at 670, 1,421, and 1,265 due to C–Cl stretching vibrations, C–H flexural vibrations of chloromethyl groups ($-\text{CH}_2\text{Cl}$), and C–H flexural vibrations of a benzene ring in CPSM, respectively. Furthermore, the characteristic absorption peak of disubstituted benzene at 828 cm^{-1} was significantly strengthened. Four new absorption bands at 3,381, 1,452, 1,380, and 1,076 cm^{-1} corresponding to hydroxyl groups ($-\text{OH}$), C–H flexural vibrations of methylene, C–H flexural vibrations of methyl, and C–O stretching vibrations of $-\text{CH}_2-\text{N}^+(\text{CH}_2\text{CH}_2\text{OH})_3$ groups were observed. The peak at 670 cm^{-1} was weakened, but it did not disappear entirely. Therefore, it could be inferred that the chemical structure of the PBO-8 resin might be as shown in Fig. 2. The BET surface area ($\text{m}^2 \text{g}^{-1}$), micro-pore area ($\text{m}^2 \text{g}^{-1}$), average pore diameter (nm), and pore volume (mL g^{-1}) of the PBO-8 resin were 14.1, 0.93, 14.0, and 0.05, respectively. Accordingly, the PBO-8 resin had been synthesized successfully.

3.2. Nitrate adsorption performance

Fig. 3(a) depicts the nitrate removal as a function of resin dosage, which shows that the nitrate removal increases with an increase in resin dosage. It revealed that the optimum amount of PBO-8 resin was 0.5 g resin/50 mL of nitrate solution, with the highest removal rate of up to 99.72% at the resin dosage of 0.8 g. Thus, the nitrate adsorption capacity of the PBO-8 resin was slightly lower than that of PBE-8 resin [18]. The lower adsorption capacity of the PBO-8 resin could be explained by the weaker alkalinity of triethanolamine. Gradual increases in nitrate adsorption by the PBO-8 resin were observed with the increase of temperature

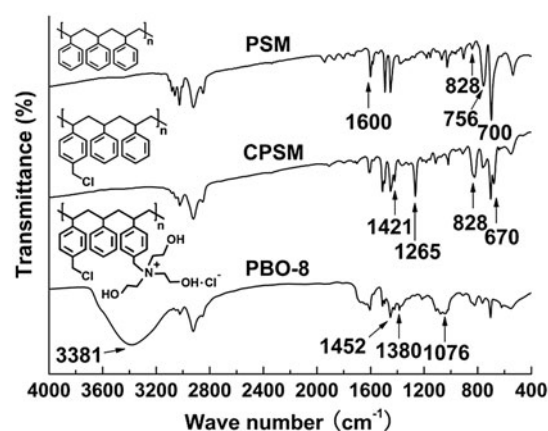


Fig. 2. FT-IR spectrum of PSM, CPSM and PBO-8 resin.

(Fig. 3(b)). The pH value of the nitrate solution was adjusted by 1 mol L^{-1} of HCl or NaOH. The amounts of nitrate adsorbed by the PBO-8 resin were 18.29, 18.26, 18.31, 16.63, and 15.55 mg g^{-1} at pH of 2, 5, 7, 9, and 11, respectively, demonstrating that a neutral pH condition was more favorable for the nitrate adsorption. This phenomenon was probably due to the presence of excess hydroxyl ions at higher pH and chloride ions at lower pH, which would compete with the nitrate for adsorption sites on the PBO-8 resin, resulting in a decreased adsorption of nitrate. As shown in Fig. 3(c), the competing anions could reduce the capacity of the PBO-8 resin to adsorb nitrate. F^- had the lowest impact on the removal of nitrate compared to CO_3^{2-} , HCO_3^- , Cl^- and SO_4^{2-} . The ordering of the influence of competing anions on the adsorption of nitrate by the PBO-8 resin follows the sequence: $\text{SO}_4^{2-} > \text{CO}_3^{2-} > \text{Cl}^- > \text{HCO}_3^- > \text{F}^-$.

3.3. Cr(VI) adsorption performance

Fig. 4(a) depicts the Cr(VI) removal as a function of resin dosage, which shows that Cr(VI) removal

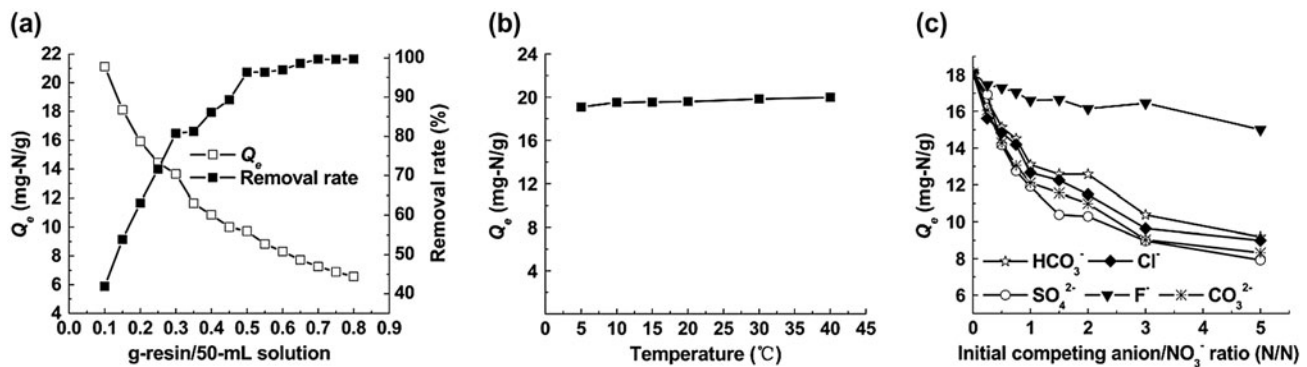


Fig. 3. Effect of resin dosage (a), temperature (b), and competing anions (c) on nitrate adsorption.

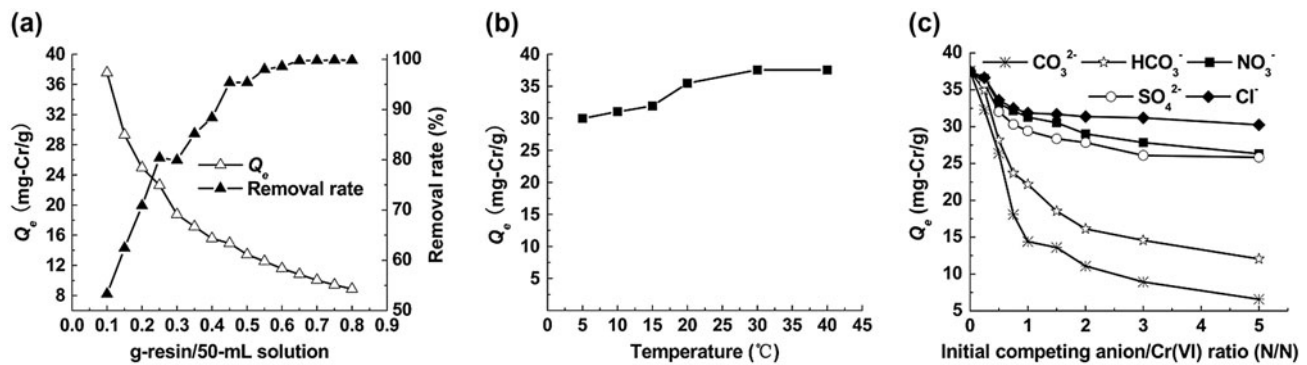


Fig. 4. Effect of resin dosage (a), temperature (b), and competing anions (c) on Cr(VI) adsorption.

increases with an increase in resin dosage. It revealed that the optimum amount of PBO-8 resin was 0.45 g resin/50 mL of Cr(VI) solution. The highest removal rate of Cr(VI) by PBO-8 could reach 99.85% at the resin dosage of 0.75 g. Fig. 4(b) shows that the increase of temperature was beneficial to the Cr(VI) adsorption reaction. The increase in temperature provided a driving force to overcome the mass transfer resistance, which accelerated the diffusivity of Cr(VI) ions from the external layer into the pores of the resin. The increase in nitrate (Fig. 3(b)) and Cr(VI) (Fig. 4(b)) adsorption by the PBO-8 resin demonstrated the endothermic nature of the adsorption. Due to the large ionic radius of Cr(VI) anions, more energy is required to overcome the mass transfer resistance in the Cr(VI) adsorption process. Thus, the temperature had a more significant influence on the Cr(VI) adsorption process of PBO-8 resin compared with the nitrate adsorption process. Additionally, the amounts of Cr(VI) adsorbed by the PBO-8 resin were 42.33, 39.82, 37.56, 22.17, and 16.05 mg g^{-1} at pH of 2, 5, 7, 9, and 11, respectively. This finding demonstrates that an acidic condition was preferred to neutral or alkaline conditions for

Cr(VI) adsorption by the PBO-8 resin, which was related to the form of Cr(VI) occurring under acidic ($\text{Cr}_2\text{O}_7^{2-}$), neutral (HCrO_4^-), and alkaline (CrO_4^{2-}) conditions. As shown in Fig. 4(c), the competing anions could reduce the adsorption capacity of the PBO-8 resin for Cr(VI). CO_3^{2-} had the largest impact on Cr(VI) removal than the other four anions. On the contrary, Cl^- had the lowest impact on the removal of Cr(VI). The existence of CO_3^{2-} and HCO_3^- had a significant influence on Cr(VI) removal by the PBO-8 resin, which could be attributed to the change in the pH of the solution. Accordingly, the influence of competing anions on the adsorption of Cr(VI) by the PBO-8 resin are as follows: $\text{CO}_3^{2-} > \text{HCO}_3^- > \text{SO}_4^{2-} > \text{NO}_3^- > \text{Cl}^-$.

3.4. Characteristics of equilibrium adsorption

Table 1 shows that the behavior of the nitrate and Cr(VI) adsorption on the PBO-8 resin can be better represented by the Langmuir isotherm than Freundlich and D-R isotherms, having recorded a higher regression coefficient. The separation factor (r) of the Langmuir isotherm was calculated to estimate

Table 1
Isotherm parameters of nitrate and Cr(VI) adsorption by PBO-8 resin

Adsorbate	Langmuir equation			Freundlich equation			D-R equation		
	Q_0	b	R^2	n	K_f	R^2	Q_0	E (kJ/mol)	R^2
Nitrate	18.69	0.157	0.991	2.512	3.378	0.951	12.68	1.306	0.821
Cr(VI)	46.72	0.178	0.990	7.722	24.049	0.855	39.36	0.766	0.592

Table 2
Thermodynamic parameters

Adsorbate	ΔG (kJ mol ⁻¹)		ΔS (kJ mol ⁻¹ K ⁻¹)	ΔH (kJ mol ⁻¹)
	277.15 K	293.15 K		
Nitrate	-3.906	-4.656	0.044	8.368
Cr(VI)	-1.079	-3.396	0.145	39.063

the type of adsorption. The r -values of nitrate and Cr(VI) adsorption on PBO-8 were in the range of 0.032–0.585 and 0.027–0.529, respectively.

The r -values of the two adsorption processes were both less than 1, which indicated that the processes of nitrate and Cr(VI) adsorption on the PBO-8 resin were both favorable. In addition, the b -value of the Langmuir isotherm was positively related to the adsorption heat. Moreover, the b -value of nitrate adsorption was lower than that of Cr(VI) adsorption, indicating that the temperature had a more significant influence on Cr(VI) adsorption process of PBO-8 resin compared with the nitrate adsorption process.

3.5. Thermodynamic studies

The Gibbs free energy changes (ΔG), enthalpy changes (ΔH), and entropy changes (ΔS) are three important parameters used to indicate the thermodynamics of a process. These thermodynamic parameters for the nitrate and Cr(VI) adsorption on PBO-8 resin were calculated at initial nitrate and Cr(VI) concentrations of 100 mg L⁻¹ according to the method described by Chabani et al. and Turki et al. [21,25], the results of which are presented in Table 2.

The absolute values of ΔG increased with the increase of temperature, indicating that a high temperature was beneficial for nitrate and Cr(VI) adsorption. The values of ΔG also showed that the adsorption process had thermodynamic feasibility and spontaneous nature. Furthermore, the positive ΔS indicated an increasing randomness at the resin/solution interface

during the adsorption of nitrate and Cr(VI) onto the PBO-8 resin. Moreover, the enthalpy change demonstrated that the nitrate and Cr(VI) adsorption process of PBO-8 were both endothermic.

In general, the type of adsorption can be determined by the value of the enthalpy change of the adsorption process. Chemisorption is viewed as a chemical bonding, and its enthalpy change is greater than the general reaction enthalpy (42 kJ mol⁻¹) [26]. By contrast, the enthalpy change of physisorption is in the range of 0–42 kJ mol⁻¹, and the mechanism of physisorption is Van der Waals interaction. In this study, the ΔH -value of the nitrate and Cr(VI) adsorption processes were all less than 40 kJ mol⁻¹. Therefore, the adsorption process of nitrate and Cr(VI) on the PBO-8 resin is related to physical adsorption with no chemical bond formation, and its main force was an electrostatic force. Furthermore, the ΔH -values of the Cr(VI) adsorption process was larger than that of the nitrate adsorption process due to the large ionic radius of Cr(VI). Thus, more energy was needed to overcome the mass transfer resistance.

3.6. Adsorption kinetic studies

As shown in Table 3, the adsorption capacity of PBO-8 for nitrate and Cr(VI) were 18.45 and 34.60 mg g⁻¹, respectively. The process of nitrate adsorption on the resin particles was fast, and a state of equilibrium was achieved up to 40 min. On the other hand, the Cr(VI) adsorption process of the resin particles was fast only at the beginning, whereby the

Table 3
Kinetic parameters of nitrate and Cr(VI) adsorption by PBO-8 resin

Adsorbate	Pseudo-first-order equation			Pseudo-second-order equation			Elovich equation		
	K_1	Q_e	R^2	K_2	Q_e	R^2	α	β	R^2
Nitrate	0.035	18.48	0.290	0.031	18.45	0.999	91.836	0.436	0.881
Cr(VI)	0.003	38.27	0.374	2.40×10^{-4}	34.60	0.995	1.241	0.190	0.886

quantity of Cr(VI) adsorbed reached half of the adsorption capacity of the PBO-8 resin within 2 h, and a state of equilibrium was attained up to 24 h. The relatively high correlation coefficients ($R^2 \geq 0.995$) indicated that the adsorption of nitrate and Cr(VI) onto the PBO-8 resin could be approximated favorably by the pseudo-second-order model. Moreover, the quantity of nitrate and Cr(VI) adsorbed by PBO-8 as estimated from the pseudo-second-order model were approximate to the experimental data.

3.7. Diffusion models and rate controlling step

Generally, the kinetics of an exchange resin is restricted by the film diffusion and intraparticle diffusion control. During the adsorption process, the rate of adsorption usually depends on $t^{1/2}$ instead of t [21,27]:

$$F_{ad} = \frac{Q_t}{Q_e} = \frac{C_0 - C_t}{C_0 - C_e} = kt^{1/2} \quad (10)$$

Assuming all the resin particles were of uniform spheres with radius, a variant Boyd model (Eq. (11)) could be applied to analyze the diffusion mechanism:

$$F_{ad} = 1 - \left(\frac{6}{\pi^2}\right) \sum_{m=1}^{\infty} \left[\left(\frac{1}{m^2}\right) \exp(-m^2 B_b t) \right] \quad (11)$$

If the F -value is higher than 0.85, then Eq. (11) can be reduced to:

$$F_{ad} = 1 - \left(\frac{6}{\pi^2}\right) \exp(-B_b t) \quad (12)$$

If the F -value is lower than 0.85, the Eq. (11) equals:

$$B_b t = 2\pi - \frac{\pi^2 F_{ad}}{3} - 2\pi \left(1 - \frac{\pi F_{ad}}{3}\right)^{1/2} \quad (13)$$

The linearity of $B_b t$ (calculated from Eqs. (12) and (13)) vs. t was used to distinguish the rate controlling step. It can be hypothesized that intraparticle diffusion is the rate-limiting step on condition that the plot is a straight line passing through the origin. Otherwise, it would be controlled by film diffusion.

As shown in Figs. 5(a) and 6(a), the nearly linear adsorption graph for the initial period of the process indicates an extremely fast uptake. During this stage, nitrate and Cr(VI) were adsorbed within a $t^{1/2}$ value of about 5 and 20 $\text{min}^{1/2}$, respectively. This phenomenon can be attributed to the rapid use of the activated adsorption sites on the surface of the PBO-8 resin. After this stage, the adsorption became slow, which may be ascribed to a slow diffusion of adsorbed nitrate or Cr(VI)

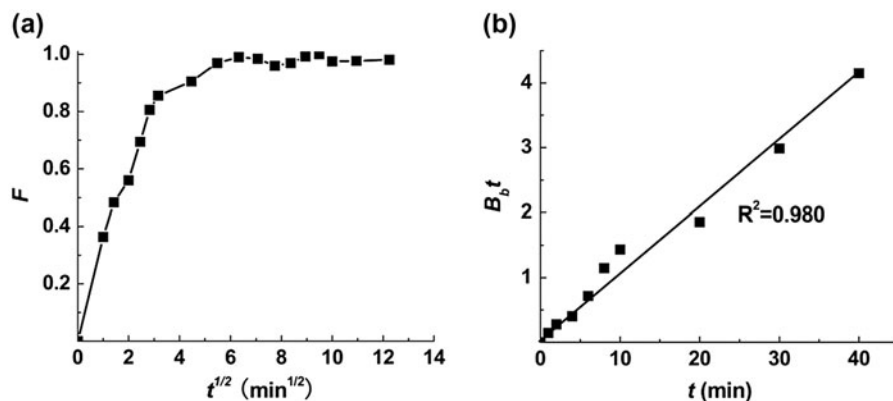


Fig. 5. Effect of $t^{1/2}$ (a) and variant Boyd model plots (b) on nitrate adsorption of PBO-8 resin.

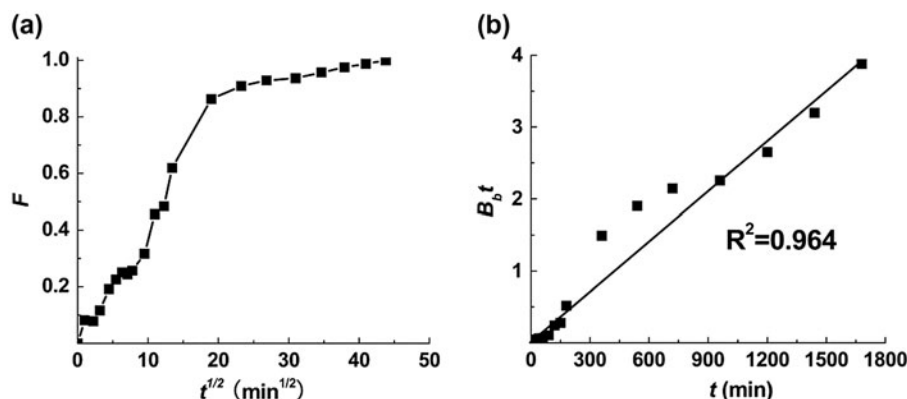


Fig. 6. Effect of $t^{1/2}$ (a) and variant Boyd model plots (b) on Cr(VI) adsorption of PBO-8 resin.

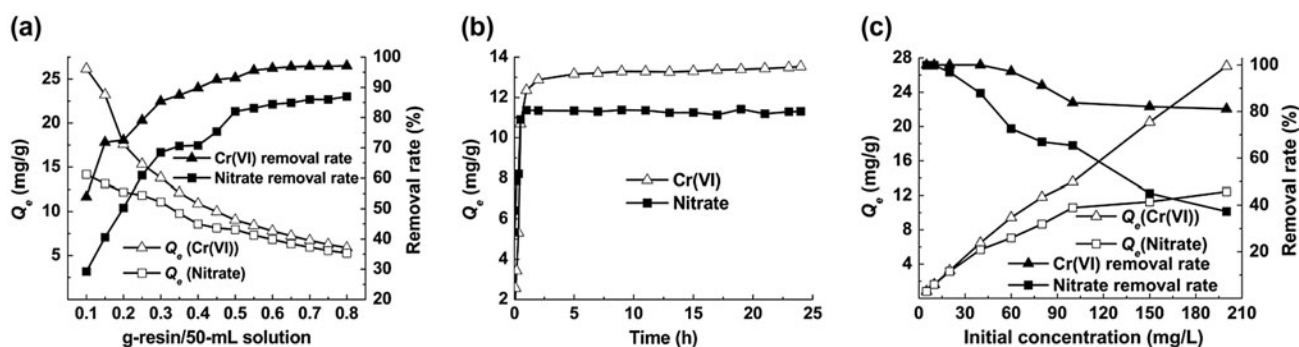


Fig. 7. Effect of resin dosage (a), time (b), and initial concentration (c) on nitrate and Cr(VI) adsorption.

from the boundary layer into the pores [21]. Moreover, the straight lines with high regression coefficients (as shown in Figs. 5(b) and 6(b)) indicated that aqueous nitrates and Cr(VI) adsorption onto PBO-8 resin were mainly controlled by the intraparticle diffusion.

3.8. Simultaneous removal of nitrate and Cr(VI)

Fig. 7(a) depicts the nitrate and Cr(VI) removal as a function of resin dosage, which shows that the nitrate and Cr(VI) removal increases with an increase in resin dosage. The optimum amount of PBO-8 resin was 0.6 g resin/50 mL of the nitrate and Cr(VI) binary solution. The highest removal rate of nitrate and Cr(VI) by PBO-8 were 86.99 and 97.09%, respectively, at the resin dosage of 0.8 g. Fig. 7(b) shows that the increase in time was beneficial to the adsorption processes. The equilibrium time for nitrate adsorption was about 40 min. The quantity of Cr(VI) adsorbed could reach 91.30% of the equilibrium adsorption

capacity of PBO-8 resin within 1 h, implying that the adsorption of Cr(VI) in a Cr(VI) and nitrate binary solution was faster than that in a single Cr(VI) solution, which could be attributed to the concentration effect. As shown in Fig. 7(c), the quantity of Cr(VI) and nitrate adsorbed increases with an increase in initial concentrations. On the contrary, the removal rate of Cr(VI) and nitrate were the opposite.

3.9. Selectivity evaluation

Generally, coexisting ions in natural waters may compete for active sites on an adsorbent, and thus, influence the application of adsorption materials in the water purification process, to some extent. Therefore, the selectivity is thought to be an important factor for the adsorbents. The selectivity coefficients of the PBO-8 resin in binary solution (Table 4) were calculated by Eq. (9) according to the experiments' results presented in Figs. 3(c) and 4(c). For nitrate removal, the adsorption selectivity of PBO-8 toward anions follow the sequence

Table 4
Selectivity coefficients of PBO-8 resin

Selectivity coefficients	Values	Selectivity coefficients	Values
$K_{\text{HCO}_3^-}^{\text{NO}_3^-}$	1.165	$K_{\text{CO}_3^{2-}}^{\text{Cr(VI)}}$	0.095
$K_{\text{Cl}^-}^{\text{NO}_3^-}$	1.042	$K_{\text{HCO}_3^-}^{\text{Cr(VI)}}$	0.873
$K_{\text{SO}_4^{2-}}^{\text{NO}_3^-}$	0.477	$K_{\text{NO}_3^-}^{\text{Cr(VI)}}$	4.019
$K_{\text{F}^-}^{\text{NO}_3^-}$	2.946	$K_{\text{SO}_4^{2-}}^{\text{Cr(VI)}}$	4.130
$K_{\text{CO}_3^{2-}}^{\text{NO}_3^-}$	0.516	$K_{\text{Cl}^-}^{\text{Cr(VI)}}$	4.449

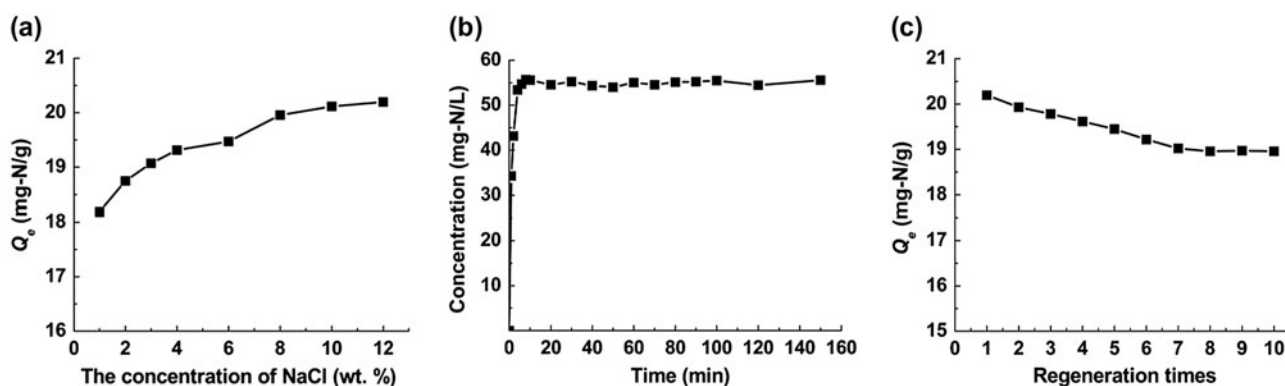


Fig. 8. Effect of salt concentration (a), time (b), and regeneration times (c) on nitrate desorption.

of $\text{SO}_4^{2-} > \text{CO}_3^{2-} > \text{NO}_3^- > \text{Cl}^- > \text{HCO}_3^- > \text{F}^-$. On the other hand, for Cr(VI) removal, the sequence of adsorption was $\text{CO}_3^{2-} > \text{HCO}_3^- > \text{Cr(VI)} > \text{NO}_3^- > \text{SO}_4^{2-} > \text{Cl}^-$. Therefore, the affinity sequence of the PBO-8 resin for anions can be concluded as $\text{CO}_3^{2-} > \text{Cr(VI)} > \text{NO}_3^- > \text{Cl}^- > \text{F}^-$. In addition, the selectivity coefficients, $K_{\text{Cr(VI)}}^{\text{NO}_3^-}$ were in the range of 0.167–0.965 with the initial nitrate and Cr(VI) concentration range of 5–200 mg L⁻¹. The values of $K_{\text{Cr(VI)}}^{\text{NO}_3^-}$ were all less than 1, which indicated that Cr(VI) was preferably adsorbed on the PBO-8 resin than nitrate. This result also could be confirmed by the b values of the Langmuir isotherms. However, the large ionic radius of hexavalent chromium anions results in its low adsorption rate. In summary, although the adsorption of nitrate and Cr(VI) on the PBO-8 resin interfered mutually, the PBO-8 resin still possesses an excellent ability to adsorb nitrate and Cr(VI) simultaneously.

3.10. Desorption studies

In practical applications, desorption is an important complement to adsorption studies to inform reusability of the resin. As the adsorption of Cr(VI) on

the PBO-8 resin is pH-dependent and lower pH is beneficial for adsorption, the desorption of Cr(VI) can be achieved using NaOH solution. The regeneration liquid for nitrate desorption was a salt solution. The results of desorption experiments are presented in Figs. 8 and 9. As shown in Fig. 8(a), the optimal concentration of salt solution for the recovery of nitrate saturated PBO-8 resin was 10–12%. With increasing NaOH concentration from 1 to 16 wt.%, a great increase in the adsorption quantity is observed (Fig. 9(a)) for Cr(VI) from 15.71 to 37.03 mg/g with the corresponding desorption efficiency of 39.28–92.58%. The high desorption efficiency indicates that ion exchange mechanism plays a leading role in the adsorption process. Fig. 8(b) demonstrates that the adsorbed nitrate can be desorbed from the active sites in the PBO-8 resin at a very fast rate (6 min) using 10% of the salt solution. However, the desorption of Cr(VI) uploaded on the PBO-8 resin required much more time (within 10 h) using 10% of NaOH solution due to the large ionic radius of Cr(VI) (Fig. 9(b)). In order to estimate the reusability of the PBO-8 resin, the adsorption–desorption cycles were repeated 10 times using the same resin. Figs. 8(c) and 9(c) shows

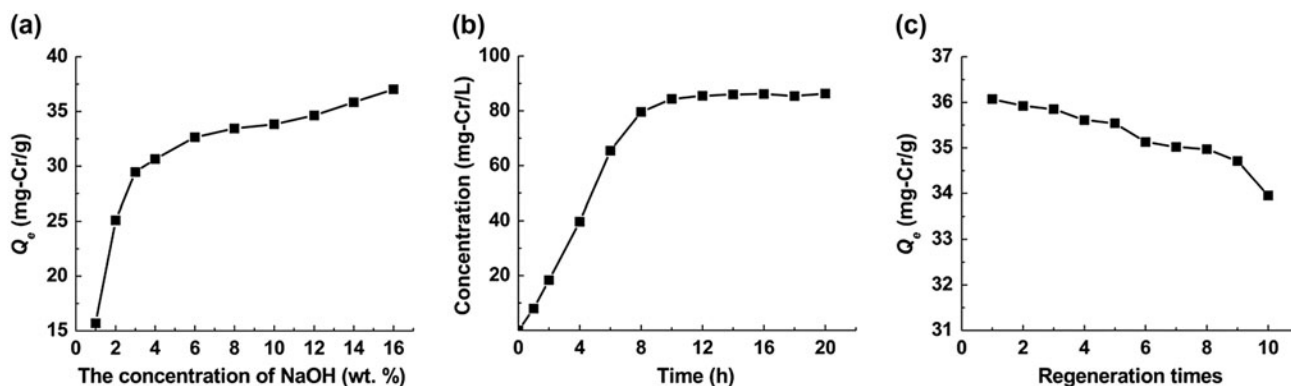


Fig. 9. Effect of NaOH concentration (a), time (b), and regeneration times (c) on Cr(VI) desorption.

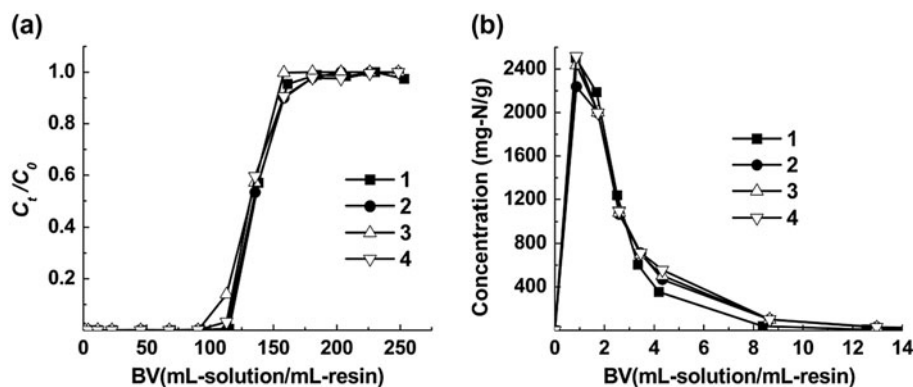


Fig. 10. Breakthrough (a) and elution curves (b) of nitrate obtained by the PBO-8 resin.

that the nitrate and Cr(VI) adsorption capacity of the PBO-8 resin was decreased by 5.82 and 5.88%, respectively, after 10 adsorption–desorption cycles, which indicate that there are no irreversible sites on the surface of the adsorbent. These results indicate that the PBO-8 resin was capable of being regenerated and repeatedly used with a great potential for the removal of nitrate and Cr(VI) from aqueous solutions.

3.11. Column adsorption and regeneration

The breakthrough and elution curves for nitrate obtained using the PBO-8 resin are presented in Fig. 10. The nitrate-saturated resin was eluted with 8 wt.% salt solution. Fig. 10(a) shows that the PBO-8 resin could repeatedly be used. The breakthrough point was 115.11 bed volumes (BV) with a breakthrough capacity of 21.19 mg-N/g-resin using simple nitrate model water. Fig. 10(b) shows the nitrate loaded onto the PBO-8 resin, which was quantitatively eluted with 25.12 BV of 8 wt.% salt solution with the corresponding desorption efficiency of 99%. However,

the performance of the dynamic adsorption and desorption of Cr(VI) by the PBO-8 resin was unsatisfactory owing to the low adsorption and desorption rate of Cr(VI). The solution to this problem is to maintain sufficient contact time between the resin and Cr(VI), which will be investigated in future research.

4. Conclusions

SEM and FTIR analyses demonstrated that the macroporous anion exchange resin, PBO-8 was synthesized successfully. The maximum capacity for nitrate and Cr(VI) adsorption at equilibrium were 21.13 and 45.02 mg g⁻¹, respectively, in single-solute solutions. The adsorption of nitrate and Cr(VI) on the PBO-8 resin interfered mutually, and the maximum capacity for nitrate and Cr(VI) adsorption at equilibrium were, respectively, decreased to 14.17 and 27.03 mg g⁻¹ in a nitrate and Cr(VI) binary solution. The existence of SO₄²⁻, Cl⁻, CO₃²⁻, HCO₃⁻, and F⁻ reduced the adsorption capacity of the PBO-8 resin for Cr(VI) and nitrate. Furthermore, the Langmuir isotherm and

pseudo-second-order models described the adsorption of nitrate and Cr(VI) by the PBO-8 resin reasonably. The three thermodynamic parameters ΔG , ΔH , and ΔS illustrated that the adsorption of nitrate and Cr(VI) on the PBO-8 resin was feasible, endothermic, and spontaneous under the examined conditions. Intraparticle diffusion was the main rate-limiting step for the nitrate and Cr(VI) adsorption processes compared with external diffusion and film diffusion. Consequently, the PBO-8 resin could potentially be applied to the purification of polluted drinking water resources.

Acknowledgment

This study is supported by the Major Science and Technology Program for Water Pollution Control and Treatment (2014ZX07305002).

Nomenclature

Q_0	— maximum adsorption capacity calculated using Langmuir model (mg/g)
Q_e	— amount of adsorption at equilibrium (mg/g)
Q_t	— adsorption capacity at time t (mg/g)
C_0	— initial nitrate concentration in the solution (mg/L)
C_e	— equilibrium concentration in the solution (mg/L)
C_t	— aqueous nitrate concentration at time t in the solution (mg/L)
V	— volume of the solution (L)
W	— mass of the dry resin (g)
b	— Langmuir constants (L/mg)
r	— separation factor of Langmuir model
K_f	— Freundlich constant ($\text{mg}^{(1-1/n)} \text{L}^{1/n}/\text{g}$)
n	— Freundlich constants
β	— activity coefficient of D-R model (mol^2/J^2)
ε	— Polanyi potential
E	— Mean free energy of adsorption (kJ/mol)
K_1	— adsorption rate constant of pseudo-first-order model (1/min)
K_2	— adsorption rate constant of pseudo-second-order model (g/mg min)
α	— initial adsorption rates of Elovich model (mg/g min)
β	— desorption constant of Elovich model (g/mg)
F_{ad}	— saturation factor of adsorption
k_{wm}	— constant of Weber–Morris model ($\text{min}^{-0.5}$)
B_{bt}	— overall rate constant
R	— universal gas constant (8.314 J/K mol)
T	— temperature (K)
t	— time (min)

References

- [1] E. Sahinkaya, A. Kilic, Heterotrophic and elemental-sulfur-based autotrophic denitrification processes for simultaneous nitrate and Cr(VI) reduction, *Water Res.* 50 (2014) 278–286.
- [2] H. Salvestrin, P. Hagare, Removal of nitrates from groundwater in remote indigenous settings in arid Central Australia, *Desalin. Water Treat.* 11 (2009) 151–156.
- [3] T. Nur, M.A.H. Johir, P. Loganathan, S. Vigneswaran, J. Kandasamy, Effectiveness of purolite A500PS and A520E ion exchange resins on the removal of nitrate and phosphate from synthetic water, *Desalin. Water Treat.* 47 (2012) 50–58.
- [4] S.N. Milmile, J.V. Pande, S. Karmakar, A. Bansiwala, T. Chakrabarti, R.B. Biniwale, Equilibrium isotherm and kinetic modeling of the adsorption of nitrates by anion exchange Indion NSSR resin, *Desalination* 276 (2011) 38–44.
- [5] J.M. van Maanen, A. van Dijk, K. Mulder, M.H. de Baets, P.C. Menheere, D. van der Heide, P.L. Mertens, J.C. Kleinjans, Consumption of drinking water with high nitrate levels causes hypertrophy of the thyroid, *Toxicol. Lett.* 72 (1994) 365–374.
- [6] A. Elmidaoui, F. Elhannouni, M.A. Menkouchi Sahli, L. Chay, H. Elabbassi, M. Hafsi, D. Largeteau, Pollution of nitrate in Moroccan ground water: Removal by electro dialysis, *Desalination* 136 (2001) 325–332.
- [7] J.L. Costa, H. Massone, D. Martínez, E.E. Suero, C.M. Vidal, F. Bedmar, Nitrate contamination of a rural aquifer and accumulation in the unsaturated zone, *Agric. Water Manage.* 57 (2002) 33–47.
- [8] Ministry of Environmental Protection of the People's Republic of China, National Groundwater Pollution Prevention Plan (2011–2020), 2011 (in Chinese).
- [9] A. Radjenovic, G. Medunic, Removal of Cr(VI) from aqueous solution by a commercial carbon black, *Desalin. Water Treat.* 55 (2015) 183–192.
- [10] J. Chung, R. Nerenberg, B.E. Rittmann, Bio-reduction of soluble chromate using a hydrogen-based membrane biofilm reactor, *Water Res.* 40 (2006) 1634–1642.
- [11] K. Huang, Y. Xiu, H. Zhu, Selective removal of Cr(VI) from aqueous solution by adsorption on mangosteen peel, *Environ. Sci. Pollut. Res.* 20 (2013) 5930–5938.
- [12] A. Al Hasin, S.J. Gurman, L.M. Murphy, A. Perry, T.J. Smith, P.H. Gardiner, Remediation of chromium(VI) by a methane-oxidizing bacterium, *Environ. Sci. Technol.* 44 (2010) 400–405.
- [13] J. Yang, L. Zhang, Y. Fukuzaki, D. Hira, K. Furukawa, High-rate nitrogen removal by the Anammox process with a sufficient inorganic carbon source, *Bioresour. Technol.* 101 (2010) 9471–9478.
- [14] J. Fang, Z. Gu, D. Gang, C. Liu, E.S. Ilton, B. Deng, Cr(VI) removal from aqueous solution by activated carbon coated with quaternized poly(4-vinylpyridine), *Environ. Sci. Technol.* 41 (2007) 4748–4753.
- [15] R. Saad, K. Belkacemi, S. Hamoudi, Adsorption of phosphate and nitrate anions on ammonium-functionalized MCM-48: Effects of experimental conditions, *J. Colloid Interface Sci.* 311 (2007) 375–381.
- [16] N. Melitas, O. Chuffe-Moscoso, J. Farrell, Kinetics of soluble chromium removal from contaminated water by zerovalent iron media: Corrosion inhibition and passive oxide effects, *Environ. Sci. Technol.* 35 (2001) 3948–3953.
- [17] B.-U. Bae, Y.-H. Jung, W.-W. Han, H.-S. Shin, Improved brine recycling during nitrate removal using ion exchange, *Water Res.* 36 (2002) 3330–3340.

- [18] Y. Ren, Y. Ye, J. Zhu, K. Hu, Y. Wang, Characterization and evaluation of a macroporous anion exchange resin for nitrate removal from drinking water, *Desalin. Water Treat.*, doi: 10.1080/19443994.2015.1085450.
- [19] Á. Bárkányi, S. Németh, B.G. Lakatos, Modelling and simulation of suspension polymerization of vinyl chloride via population balance model, *Comput. Chem. Eng.* 59 (2013) 211–218.
- [20] S. Samatya, N. Kabay, Ü. Yüksel, M. Arda, M. Yüksel, Removal of nitrate from aqueous solution by nitrate selective ion exchange resins, *React. Funct. Polym.* 66 (2006) 1206–1214.
- [21] M. Chabani, A. Amrane, A. Bensmaili, Kinetic modelling of the adsorption of nitrates by ion exchange resin, *Chem. Eng. J.* 125 (2006) 111–117.
- [22] L. Zhu, Y. Deng, J. Zhang, J. Chen, Adsorption of phenol from water by N-butylimidazolium functionalized strongly basic anion exchange resin, *J. Colloid Interface Sci.* 364 (2011) 462–468.
- [23] F.-C. Wu, R.-L. Tseng, R.-S. Juang, Characteristics of Elovich equation used for the analysis of adsorption kinetics in dye-chitosan systems, *Chem. Eng. J.* 150 (2009) 366–373.
- [24] O. Karnland, M. Birgersson, M. Hedström, Selectivity coefficient for Ca/Na ion exchange in highly compacted bentonite, *Phys. Chem. Earth, Parts A/B/C* 36 (2011) 1554–1558.
- [25] T. Turki, S. Hamouda, R. Hamdi, M. Ben Amor, Nitrates removal on PUROLITE A 520E resin: Kinetic and thermodynamic studies, *Desalin. Water Treat.* 41 (2012) 1–8.
- [26] J. Yang, M. Yu, T. Qiu, Adsorption thermodynamics and kinetics of Cr(VI) on KIP210 resin, *J. Ind. Eng. Chem.* 20 (2014) 480–486.
- [27] J. Ma, Z. Wang, Z. Wu, T. Wei, Y. Dong, Aqueous nitrate removal by D417 resin: Thermodynamic, kinetic and response surface methodology studies, *Asia-Pac. J. Chem. Eng.* 7 (2012) 856–867.